UCRL-85697
PREPRINT

# Fusion-Reactor Aspects of the Compact Torus

Charles W. Hartman

This paper was prepared for presentation at
the Intern. School of Fusion Reactor Technology's
Course on Unconventional Approaches to Fusion
Erice, Italy, 16-27 March, 1981

March 11, 1981

# FUSION-REACTOR ASPECTS OF THE COMPACT TORUS*

Charles W. Hartman

Lawrence Livermore National Laboratory
University of California
Livermore, CA 94550

ABSTRACT

This paper summarizes several studies of fusion reactors based on the compact torus (CT). A wide variety of reactor configurations can be projected within present understanding of the possible types of CT and their macroscopic stability and confinement properties. Three types of CT are considered here, the field-reversed-configuration having $B_{Toroidal} = 0$, the Spheromak with $B_T \neq 0$, and CT's formed with particle rings. For each type, either fixed or moving-ring possibilities are offered along with pulsed or steady operation. In all cases the CT configuration lends itself to simplified blanket and coil design. In certain, important cases a reactor-scale CT is predicted to produce small unit power (10-100 $MW_e$) facilitating small-scale pilot plants and eventual modularity.

*Work performed under the auspices of the U.S. Department of Energy by the Lawrence Livermore National Laboratory under contract number W-7405-ENG-48.

## INTRODUCTION

The purpose of this paper is to review some fusion reactor possibilities based on the compact torus (CT) confinement configuration shown in Fig. 1. The general advantages of the CT, as discussed in an accompanying paper,[1] are that reactor-related aspects of toroidal plasma confinement are combined with a basically simple, open, external field. No conductors or blankets link the torus. The external field provides natural diversion of the plasma and can be generated with simple coils or possibly eddy currents in nearby walls. Since the toroidal plasma ring is free to move along the external B, reactor configurations based on a moving ring are also possible. Finally, because the basic fusion unit is a compact torus, it can be small, with possibly $P_e$ = 10-100 MWe.

The plasma physics basis for CT reactor projections is derived from MHD stability theory and experimental observations of macrostability, and from postulated transport scaling or scaling of related devices (tokamak and diffuse, toroidal pinch). A central issue, on which different reactor projections can be based, centers on the observed macrostability of certain CT's (reversed field theta-pinch,[2] $B_{Toroidal} = 0$) in apparent contradiction with MHD stability theory.[3] Although the conflict may be resolved by inclusion of finite-ion-larmor radius (FLR) effects in the theory, scaling assumptions to reactor conditions may or may not invoke FLR.

Two basic approaches have evolved, depending on the scaling assumptions made: (1) the observed stability is used as a basis, and FLR effects are scaled holding $S = hR/a_i$; constant where $h = h(L/R)$ is a geometrical form factor and R is the CT major radius , or (2) MHD stability theory is assumed to hold, requiring $B_T \neq 0$ for shear stabilization. The CT configuration assumed in (1) will be referred to in this paper as a field-reversed-configuration (FRC). It has $B_T = 0$, $\beta = 1\text{-}2$, and in experiments, is characterized by $S \leq 30\text{-}50$ with the upper limit set by experimental parameters, not stability. The CT configuration of (2) for which $B_T = 0$, here referred to as a Spheromak, is nearly force-free with a maximum predicted stable local $\beta$ or $\beta_{max} = 0.05$. Finally, a third CT configuration, discussed later, is based on circulating energetic particles.

Among the three possible CT configurations, continuous or pulsed, fixed or moving ring, and ignited or driven reactors can be projected presenting quite a formidable array of possibilities! In general, continuous operation requires a mechanism for sustaining the plasma current which, even for ignition, limits the maximum $Q = P_{fusion}/P_{in}$ to $Q \leq P_{fusion}/P_{current\ drive}$. Pulsed systems rely on the fact that the magnetic diffusion time

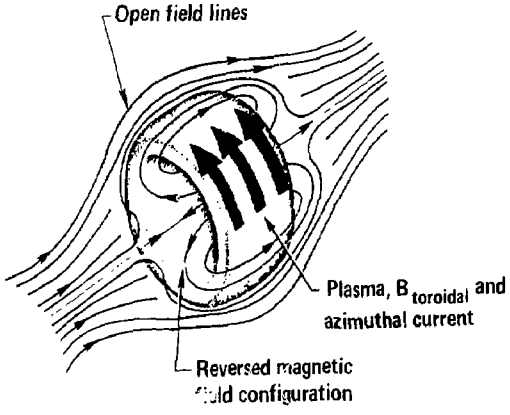


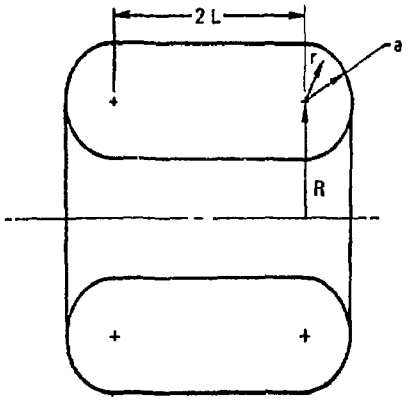


Fig. 1 Compact torus field configuration and approximate geometry used in this paper.

$\tau_B$ is usually long $\tau_B >> \tau_{Lawson}$ and Q is determined by inefficiencies in ring formation and recovery. Two potentially useful possibilities arise in the moving ring reactor; separation of the ring formation and recovery parts of the reactor from the fusion region, with attendant simplifications, and reduction of the average power incident on the first wall.

In the following discussion, various reactor designs will be considered in the broad categories FRC, Spheromak, and particle-ring CT based reactors.

## CT REACTORS BASED ON THE FRC ($B_T = 0$)

The FRC, CT is characterized by $B_T = 0$ and $\beta = 1$-2. Macroscopic stability is assumed to result from FLR effects (although possibly other kinetic effects may be important) characterized by the parameter[4] $S = R/a_i < h(L/R)\ S_0$ for stability. Heuristically, FLR importance is measured by the diamagnetic-drift frequency $\omega^* = \omega_{ti}\ a_i/a^2$ compared to the MHD growth rate $\gamma \simeq L/v_{ti}$,[5] ($\beta = 1$) so that stabilization can be important for $\omega^* \sim \gamma$ or $S < (L/a)\ S_0$. An approximate theory[6] suggests $S_0 \sim$ several so that stability

might be expected for $S \sim$ several x L/a consistent with FRC experiments.[7] The quantity S may be estimated for FRC with $L/a >> 1$, $T_e \simeq T_i$ to be

$$S = \frac{a}{a_i}\left[\frac{n\,a^2}{5 \times 10^{14}\ (cm^{-1})}\right]^{1/2}.$$

Holding $L/a \sim S$, $\beta = 1$, and $R \sim$ a constant, reactor scaling considerations give,

$$n \propto S^2/R^2$$
$$B \propto S/R$$
$$P_{wall} \propto n^2R \propto S^4/R^3$$
$$P_{total} \propto S^4/R.$$

For $S \simeq 5$-15, the total fusion power $P_{total}$ tends to be small unless R is also small. Choosing small R leads to large n and high power density but excessive wall power $P_w$ unless the walls are distant or the FRC is translated. To achieve larger total power for stationary FRC's a modular reactor can be considered with a stacked series of rings.

### Fixed Ring FRC Reactor

A fixed-ring, field-reversed-mirror (here FRC) pilot reactor has been considered by G. Carlson et al.,[8,9,10] and is shown in Fig. 2. For the reactor, a single DT ring would be maintained by injection of 200 keV neutral beams. Using the

Table 1. Input Parameters[10]

| | |
|---|---|
| $E_{in}$ | 200 keV |
| j | 3 |
| M | 1.25 |
| R/a | 2 |
| L/a | 2 |
| S | 5 and 7 |
| $\beta$ | 2.81 |

Table 2. FRM Plasma Parameters[10]

| | S = 5 Plasma | S = 7 Plasma |
|---|---|---|
| a (cm) | 6.1 | 11 |
| Volume (litre) | 33 | 200 |
| $B_0$ (T) | 4.8 | 4.6 |
| $I_{plasma}$ (MA) | 3.4 | 5.9 |
| | 2.8 | 2.8 |
| $n_0$ ($10^{15}$ cm$^{-3}$) | 1.3 | 1.0 |
| n ($10^{14}$ cm$^{-3}$ | 9.5 | 7.2 |
| $E_p$ (keV) | 100 | 150 |
| $T_e$ (keV) | 35 | 60 |
| $E_{inj}$ (keV) | 200 | 200 |
| $I_{inj}$ (A) | 22 | 16 |
| $P_{inj}$ (MW) | 4.4 | 3.2 |
| $P_{fus}$ (MW) | 22 | 42 |
| Q | 5 | 13 |

input parameters of Table 1, FRC parameters given in Table 2 were obtained numerically using a zero-dimensional model of particle and heat flows. For Table 2, ion heat flow was taken to be classical, electron heat flow 5X classical, the particle time was taken to be $\tau_n = S^2 \tau_{ii}$ where $\tau_{ii}$ is the ion-ion scattering time, and a fraction f = 0.25 of the $\alpha$-particle energy is deposited in the plasma. (Single particle calculations[11] predict ignition for S > 15.) The first wall loading for this design is 6.1 MW/m$^2$.

The FRC in the pilot reactor above is assumed to correspond roughly to a spherical Hill's vortex[12] equilibrium in a uniform external field. Weak mirror and quadrupole fields are assumed to stabilize the ring. The ring current is assumed to

be maintained by rotation of the plasma in the presence of the quadrupole field[13] or by a nonrotating ion species such as the fusion α-particles or injected ions.[14]

Similar calculations of elongated FRC rings have also been made with results shown for reference in Tables 3, 4, and 5. To maintain large L/a, external, equilibrium fields which are stronger at the midplane of the ring than at the ends are required. A detailed study of macrostability of the rings for this case has not been made however.

To start up the reactor it is assumed that a FRC is injected from the ends along the equilibrium guide field. Several possible means of forming and injecting the FRC have been considered with the magnetized, coaxial gun shown in Fig. 3 investigated most thoroughly. Table 6 provides a comparison of the present experimental gun parameters of the Beta II experiment[15] at LLNL and scaled-up guns required for the S = 5 and 7 cases discussed earlier. Experiments on gun scaling have not revealed any basic limit to scale up to 0.5 MJ thus-far.[16] Further, it may be possible to start up the FRC with a "seed" field reversal which is brought up to full level by the current-drive mechanism.

Moving Ring, FRC Reactor

Potential advantages of a moving-ring reactor cited earlier are in separation of the ring formation, heating, and recovery parts of the reactor from the main burn region, and greater

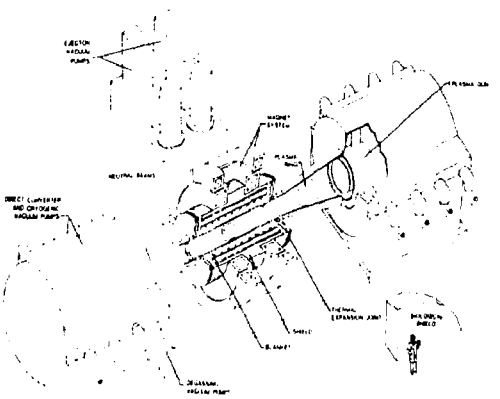

Fig. 2 Schematic of a fixed-ring, field-reversed-mirror pilot reactor.[10]

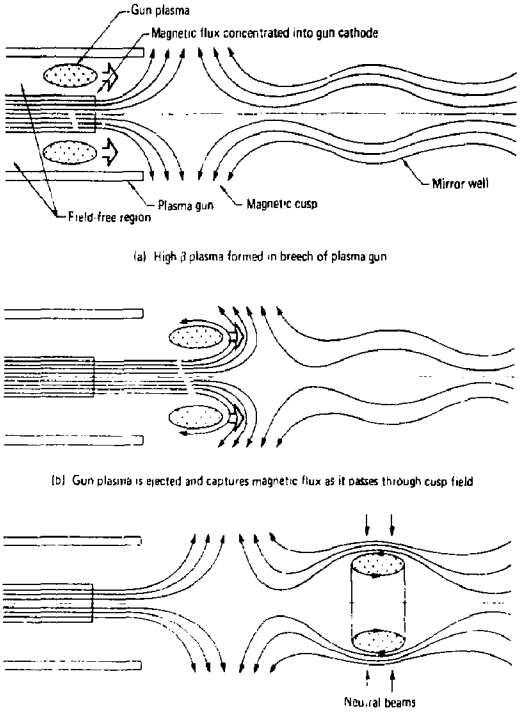


Fig. 3 Magnetized, coaxial plasma gun for CT reactor startup.[8]

control of wall loading. Additionally, compressional heating and decompressional recovery both involve inductive coupling to the ring and can be quite efficient. Separation of the burn region, which can be rather simple, from the formation and recovery regions, allows greater freedom of design for neutron considerations and consequent simplifications. A schematic of a moving ring reactor is shown in Fig. 4.

Start-up of the fixed ring reactor is quite similar to ring formation and recovery here. Compression of the ring by a moving magnetic mirror is illustrated in Fig. 5. To avoid

Table 3. Reference Case Plasma Parameters[8]

| | |
|---|---|
| Injection energy | 200 keV |
| $S = a/a_i$ | 5 |
| a | 0.07 m |
| R/a | 2 |
| L/a | 6 |
| | 1.5 |
| Alpha-particle energy deposition | 10% |
| Particle confinement | ion-ion collision time |
| $n_0$ | $6.5 \times 10^{20}$ $m^{-3}$ |
| Density profile | cubic |
| $T_e$ | 31 keV |
| $E_p$ | 96 keV |
| $B_0$, VAC | 4.1 T |
| Fusion power | 20 MW/cell |
| Q | 5.5 |

Table 4. Reference Case Cell Parameters[8]

| | |
|---|---|
| Cell Length | 2.0 m |
| First wall radius | 0.73 m |
| Average first wall neutron loading | 1.7 $MW/m^2$ |
| Peak first wall neutron loading | 2.6 $MW/m^2$ |

Table 5. Power Balance and Cost for Reference Case[8]

| | |
|---|---|
| Injected power | 40 MW |
| Fusion power | 220 MW |
| Blanket energy multiplication | 1.2 |
| Direct conversion efficiency | 0.5 |
| Thermal conversion efficiency | 0.4 |
| Gross electric power | 136 MW |
| Injection system efficiency | 0.74 |
| Power recirculated to injectors | 54 MW |
| Power recirculated to copper coils | 8 MW |
| Net electric power | 74 MW |
| Recirculated power fraction | 0.46 |
| System efficiency | 0.29 |
| Direct capital cost | $89 M ($1210/kWe) |

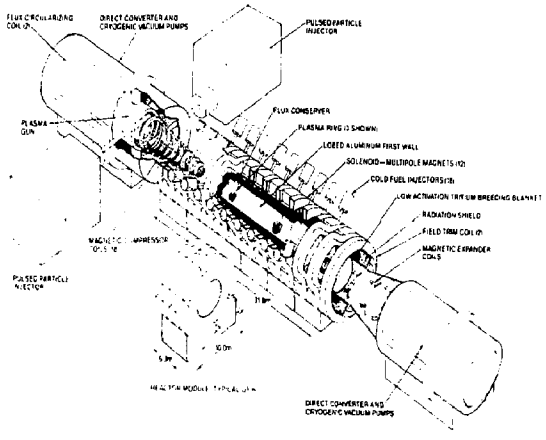


Fig. 4 Schematic of a moving ring, field-reversed-mirror prototype reactor.[9]

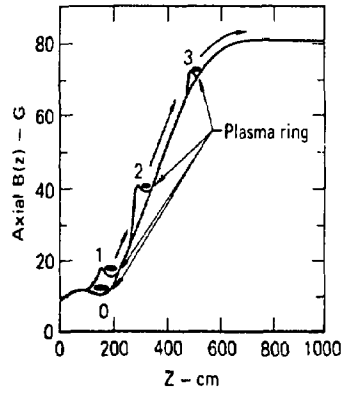


Fig. 5 Conceptual sequence of simultaneous compression and translation of initial plasma ring in solenoidal, fringing-field compressor section.

tilting instability it may be necessary to spin the ring[17] or add some axis-encircling particles although these possibilities have not been examined in detail. Alternatively, it may be possible to design a system in which the ring axis is normal to the direction of motion[18] as shown in Fig. 6. Stability against the tilting instability would be provided by the nearby conducting walls.[19]

A. C. Smith et al.,[20] have considered a prototype moving-ring, field-reversed-mirror reactor shown in Fig. 4 and summarized in Table 7. Plasma rings are formed with a magnetized, coaxial, plasma gun and compressed in 2-5 msec from R = 150 cm, $T_i$ = 3 keV to R = 30 cm. $T_i$ = 75 keV. In order to achieve ignition, S = 16 was considered. A 0-D numerical model was used to calculate the burn history. To make the

Table 6. Comparison of Beta II Gun and Pilot FRM Reactor Gun[10]

| | Beta II Gun | S = 5 | S = 7 |
|---|---|---|---|
| Center conductor radius, $R_1$, cm | 7.5 | 85 | 85 |
| Outer conductor radius, $R_2$, cm | 15 | 115 | 115 |
| Length, $l_g$, cm | 150 | 150 | 150 |
| Voltage, V, kV | 40 | 59 | 330 |
| Output energy, $U_g$, MJ | 0.2 | 3.2 | 17.9 |
| Flux in center conductor, $\psi_{poloidal}$, Wb | 0.07 | 0.24 | 0.755 |
| Poloidal B in center conductor, $B_p$, T | 4.0 | 0.104 | 0.33 |
| Guide field at gun muzzle, T | 0.2-0.4 | 1.1 | 1.05 |

Table 7. Moving-Ring, Field-Reversed-Mirror, Prototype Reactor Parameters[20]

$n = 10^{15}$ cm$^{-3}$
$T_i$ = 75 keV (initial)
$B_0$ = 6.5 T
S = 11 - 22
$\tau_E = (a/a_i)^2 \tau_{ii}$
$\tau_n = \tau_E$
R = 31 - 53 cm
L = 2R
$I_{ring}$ = 12.4 MA
$P_{fusion}$ = 320 MW/ring
$P_{net}$ = 376 MW (3 rings)
$P_{circulating}/P_{gross}$ = 0.13
$P_{wall}$ = 2.75 MW/m$^2$

fusion power output of the ring constant, "cold," 3 keV or so ions are injected periodically, raising n and decreasing T. The results are shown in Figs. 7 and 8. The ring velocity in the burn section is held constant by balancing eddy-current drag and a weak, accelerating gradient in the external field. The first wall of the burn section is taken to be high purity aluminum with wall loading of 6.3 $MW/m^2$ peak, 1.1 $MW/m^2$ minimum, and 2.75 $MW/m^2$ average. The rings pass by each 0.5 sec. The net power out, 376 MW, of this design is considered somewhat high for a prototype and further iterations are planned.

A moving ring CT reactor based on the FRC has been studied by Hagenson and Krakowski[21] and is summarized in Table 8. The ring is produced by a field-reversed θ-pinch with $T_i$ = 1.6 keV and compressed radially by 2.9 and axially by 1.9 to give $T_i$ = 8 keV for ignition. The ring velocity during burn is decreased, $v \propto P/r_{wall}$ as α-particle heating causes the ring to expand, decreasing the fusion power. The burn is terminated by α-particle buildup and ring expansion. For rings injected each 5.8 sec (to give 2 $MW/m^2$ wall loading) a thermal output of 1050 MW is obtained.

## CT REACTORS BASED ON THE SPHEROMAK ($B_T \neq 0$)

The Spheromak reactor[22] is based on ideal and resistive MHD stability of a CT having an internal toroidal field. Stability considerations indicate that the overall shape must be sufficiently oblate and with a surrounding conducting shell, and that the overall configuration must be nearly force-free. The calculated maximum local β limit is $\beta_{max} \simeq 2\text{-}4\%$ using the Mercier criterion for shear-stabilized interchange modes. Although $\beta_{max}$ is somewhat low, β measured in terms of the field strength at the external field coil is $\langle\beta x\rangle_{coil}$ = 13-25% as compared with a representative tokamak where $\langle\beta x\rangle_{coil}$ = 1.3-2.5%.

Two reactor embodiments of the Spheromak have been considered, a large, ignited reactor with resistively decaying currents, and a small, steady-state reactor having two ion-energy components. Table 9 gives representative parameters of the large reactor. In this reactor model the energy multiplication factor $Q_M$ is based on dissipative loss of the magnetic field energy. If the plasma energy confinement time follows neoclassical transport, ohmic heating power alone is sufficient to heat to ignition. If, on the other hand, tokamak scaling determines plasma energy loss, auxiliary heating to ignition is necessary but energy loss after ignition is sufficiently small so that $Q \simeq Q_M$.

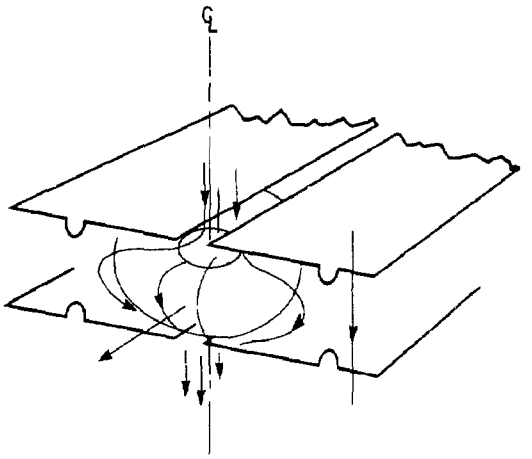


Fig. 6 Conceptual schematic of a "frisby"-type moving ring reactor. The symmetry axis is orthogonal to the direction of motion and the surface of conducting stabilizing plates.

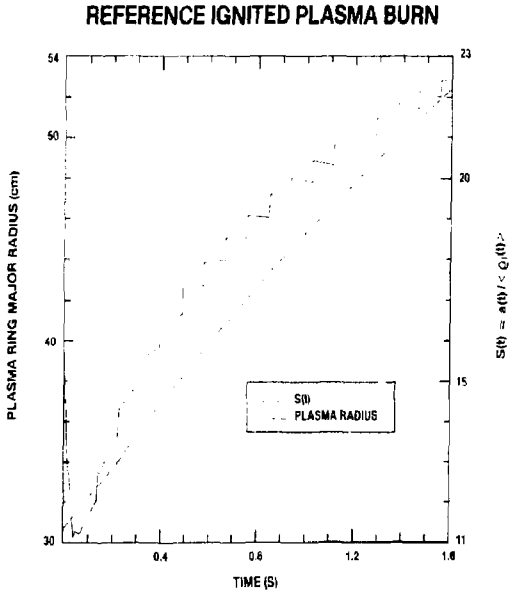


Fig. 7 Plasma radius R, and S parameter vs time for the moving-ring, field-reversed-mirror reactor.[20]

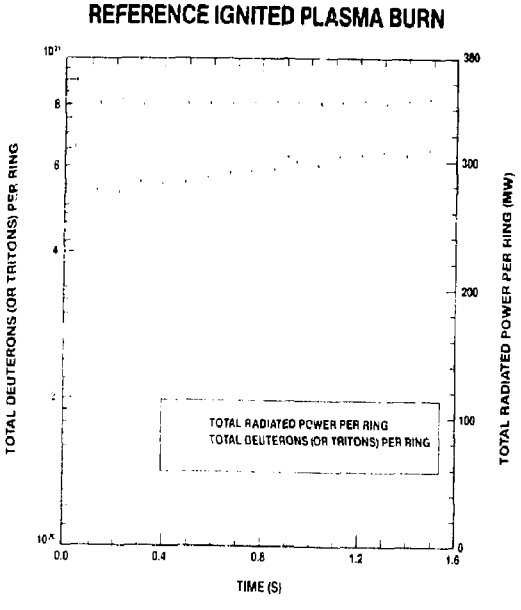


Fig. 8 Total power and particle inventory vs time for the moving-ring, field-reversed-mirror reactor.[20]

Table 8. C.T. Reactor Based on the Field-Reversed Theta Pinch[21]

$n = 10^{15}$ cm$^{-3}$
$T_i$ = 10-15 keV
$B_0$ = 0 (Eddy current supported)
$\tau_E = 200\ \tau_{Bohm}$
$\tau_n = \infty$ (Batch Burn)
R = 100 cm
L = 1000 cm
$\tau_{injection}$ = 5.8 s
$\tau_{burn}$ = 2 s
$P_{fusion}\ \tau_{burn}$ = 6180 MJ
$P_{net}$ = 328 MW ($\tau_I$ = 5.8 s)
$P_{circulating}/P_{gross}$ = 0.13
$P_{wall}$ = 2 MW/m$^2$

Table 9. Representative Parameters for a Large Spheromak Ignition Reactor With Resistively Decaying Currents[22]

| | |
|---|---|
| Minor radius | 125 cn |
| $B_{to}$ | 120 kG |
| $B_{edge}$ | 40 kG |
| I | 70 MA |
| $T_e - T_i$ | 20 keV |
| n | $2\ 10^{14}$ cm$^{-3}$ |
| $<\beta^*>_0$ | 2% |
| M | ~10 min |
| Magnetic energy storage | ~$2\ 10^3$ MJ |
| Fusion yield per pulse | ~$2\ 10^5$ MJ |
| $Q_M$ | ~$10^2$ |
| Pwall | ~5 MW/m$^2$ |

Representative parameters of a small Spheromak TCT reactor are given in Table 10. Here it is argued by the authors of Ref. 22 that, for a single ion component, the Q for resistivity losses,

$$Q_R = 40\ \epsilon_I \beta^2 I^2 T_e^{3/2}$$

is unlikely to be large for I = 10 MA since both $\beta$ is small (in contrast to the FRC reactor discussed earlier where $\beta \simeq 1$) and $\epsilon_I$, the efficiency of current drive, is likely to be small. If neutral beams are assumed to sustain the current, then a TCT (Two Ion Component Torus) reactor can provide a more optimum design (as shown) for steady state. It is interesting to note that a similar size TCT reactor could achieve Q > 1 even with Bohm diffusion.

An interesting possibility for continuous Spheromak operation is to increase $T_e$ in $Q_R$ above by providing the current with a small fraction of energetic electrons (as discussed later). If reasonable $\epsilon_I$ can be achieved in this case, high Q, small, continuous, Spheromak reactors may be possible.

PARTICLE-RING CT REACTOR

Experiments using relativistic electrons[23] have shown that reversed-field configurations can be formed which are macroscopically stable and decay with a lifetime established by classical scattering of the energetic electrons. The use of particle rings (gyroradius ~R) for a CT reactor can provide possibilities for current drive, plasma heating, stabilization, and confinement.

Although relativistic electrons have been successfully used to form CT rings, extrapolation to reactor scale with $B_T = 0$ is impractical because of synchrotron radiation. A simple argument can be made by estimating the maximum fuxion $Q_{max} = P_{fusion}/P_{synchrotron}$. Noting the total power radiated by an electron is,[24]

$$T = \frac{e^2 \omega_b^2 \gamma^2}{6\pi \epsilon_0 c} \text{ watts (MKS)}$$

the total power radiated by an electron ring undergoing simple gyro-orbit motion is

$$P_e = \frac{1}{3} \frac{I_e e}{R \epsilon_0} \left( \frac{R\omega_b}{c} \right)^4$$

where $\omega_b = (e/m_0) B_0 = \gamma c/R$, $B_0 \simeq \mu_0 I_e/4R$ is the external field, $I_e = N_e ec/2\pi R$ is the ring current, $N_e$ is the total number of ring electrons, and R is the ring radius. It is assumed that $B_{z0}$ due to the ring is $\sim -2\ B_0$ (200% reversal) and that $\gamma >> 1$. Elimination of $\omega_b$ gives,

$$P_e \geq 7.3 \times 10^{-24} \frac{I_e^5}{R^2} \text{ watts/ring}$$

where the $\geq$ sign reflects neglect of transverse Betatron motions of the ring electrons. The fusion power is, approximately,

$$P_{fusion} \simeq 2\pi R \pi a^2 \frac{\overline{n^2} \langle \sigma v \rangle}{4} e E_{fus}$$

Table 10. Representative Parameters for a Small Spheromak TCT Reactor With Beam-Driven Currents[22]

| | |
|---|---|
| Minor radius | 25 cm |
| $B_{To}$ | 120 kG |
| $B_{edge}$ | 50 kG |
| I | 6 MA |
| $T_e \sim T_i$ | 20 keV |
| n | $2\ 10^{14}$ cm$^{-3}$ |
| Plasma $\langle \beta^* \rangle_0$ | 2% |
| $\tau_M$ | 20 s |
| $V_{beam}$ | 150 keV |
| $I_{beam}$ | 100 A |
| Beam $\langle \beta^* \rangle_0$ | 4% |
| Fusion power | 40 MW |
| $Q_R = Q_{TCT}$ | 2.5 |

for a 50-50 DT ring. Now, the maximum plasma pressure which can be sustained is given by the Bennett relation[25]

$$I_{total}^2 = \frac{16\,\pi^2 e}{\mu_0}\, na^2\, T$$

where $T_e = T_i$ and $B_T = 0$. Using $\overline{n^2} = n^2$ and combining gives

$$P_{fusion} \quad 3.3 \times 10^{-20}\, \frac{R I_{total}^4}{a^2}$$

where $E_{fus} = 17.6$ MeV, $\langle \sigma v \rangle = 10^{-18}$ cm$^2$/s, and $T = 20$ keV.

The maximum Q is,

$$Q_{max} = 4500\, \frac{R^2}{a^2}\, \frac{I_{total}^4}{I_e^5} \quad .$$

If $I_e$ is small enough, $Q_{max}$ can be made large however any advantages of the high energy electrons are lost. If $Q_{max} = 10$, $R/a = 2$, and $I_{tot} = 10^7$ A, then,

$$\frac{I_e}{I_{total}} = 0.2 \ll 1 \quad ,$$

and for larger $I_e/I_{total}$ $Q_{max}$ rapidly decreases to $Q_{max} < 1$.

Energetic electrons may, however, be useful if there is a toroidal field and if their energy is not too high. In this limit, the energetic electrons flow mostly along B to form a nearly force-free Spheromak configuration[26,27] for which the maximum stable $\beta$ is $\beta_{max} = 0.1$.[28] Following the above argument, the Q associated with synchrotron radiation becomes,

$$Q_{max} = 5.3 \times 10^{-12}\, \frac{R^2}{a^2}\, \frac{I^3 \beta^2}{\gamma^4}$$

which, for $R/a = 1$, $\beta = 0.1$, $I = 10$ MA, and $Q_{max} = 1$ gives $\gamma = 85$ or $E_{max} = 44$ MeV.

If the electron energy is less than 44 MeV, synchrotron radiation rapidly becomes small and a broad range of energy is available for a high energy "tail" of the electron distribution to carry the plasma current with minimized classical dissipation.

As an alternative to energetic electrons, protons, deuterons, or tritons have been considered by Fleishmann and

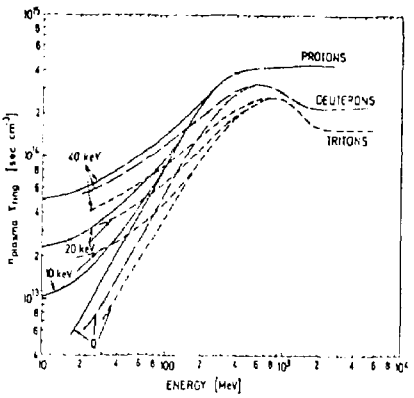


Fig. 9 Estimated ion ring lifetimes, $\tau_r$ for various ion species in plasma of density, n, and various electron temperatures, kT.[29]

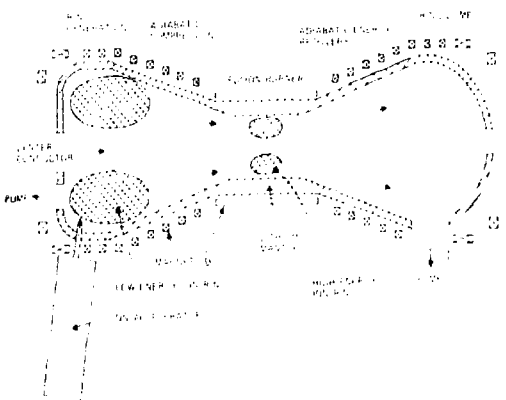

Fig. 10 Schematic of ion ring reactor with adiabatic compression.[29]

Kammash for an ion-ring-compression CT reactor.[20] If the ion velocity is sufficiently high, $v_i > v_{te}$, the rings can act as a current source in contrast to low-energy ion beams which generate no net current.[30] Taking protons, for example, the energy range of interest in a $T_e$ = 20 keV plasma for current generation is $E_p \simeq 100$ MeV. For still higher $E_p$, electron

drag continues to be reduced until above about 250 MeV, the ring lifetime is limited by nuclear scattering as shown in Fig. 9.

Defining a power gain factor Q,

$$Q = \epsilon_a \epsilon_t \eta P_{fus}/P_{ring}$$

arguments similar to those given earlier are given to get, what is argued an underestimated Q,

$$Q = (1.2 - 2)\, \epsilon_a \epsilon_t \eta$$

for the Ion-Ring-Compressor reactor. Here the ring particles are taken to have 300 MeV/nucleon and, $P_{ring}$ is the ring power lost to drag, $\epsilon_a$ is the accelerator efficiency, $\epsilon_t$ the trapping efficiency, $\eta$ the thermal converter efficiency, and $\beta$ is taken to be $\beta = 0.5$. It is argued that the trapping efficiency $\epsilon_t$ is too low for direct injector of 300 MeV particles but with injection at 30 MeV followed by compression adequately high $\epsilon_a \epsilon_t = 50\%$ can be ootained.

Table II. Typical Parameters for Ion-Ring Compressor Reactor Concept[20]

| | Burn Chamber | Compression Chamber |
|---|---|---|
| Deuteron energy (MeV) | 300 | 30 |
| Total fast-ion charge (C) | 1.5 | 1.5 |
| Major ring radius (m) | 3 | 10 |
| Radial ring thickness (m) | 3 | 10 |
| Axial ring length (m) | 4.5 | 15 |
| Temperature (keV) | 20 | Low |
| Density ($10^{20}/m^3$) | 0.63 | 0.1 |
| Fusion power per ring (MW) | 300 | 0 |
| Total energy per ring (MJ) | 540 | 50 |
| Ring lifetime (s) | 5 | 0.1 |
| External axial magnetic field (T) | 1.4 | 0.14 |
| Magnetic field at ring radius (T) | 0.67 | 0.20 |
| Axial current (MA) | 10 | 10 |
| First-wall radius (m) | 4.5 | 15 |
| First-wall loading ($MW/m^2$) | 2.3 | 0.1 |
| Compression time (s) | - | 0.2-0.5 |
| Duty cycle | 0.8-0.9 | - |
| Ring energy gain, Q | 3[a] | - |

[a]More recent estimates (Ref. 195) indicate the Q values in the range of 5 to 10 may be possible.

A cross section of the Ion-Ring-Compressor reactor is shown in Fig. 10, and estimated parameters are given in Table II. As with the FRC moving-ring reactors, the rings are formed and compressed to fusion conditions, passed through a burner section, and recovered by the inverse of formation.

## SUMMARY

It is evident from the foregoing discussion that a large number of reactor possibilities can be based on the CT. These studies must, however, be considered as preliminary since a sufficiently large data base is not yet available on the actual performance of the CT as a plasma confinement configuration. Depending on assumptions, a large range of output power may be possible including, especially, small units which, in pilot operation, may be rapidly iterated to achieve optimum system performance and for full-scale operation may be linked as individual modules.

Basic simplifications over conventional toroidal-reactor designs were found to be introduced with the CT confinement configuration. For stationary ring reactors a difficulty associated with maintaining the plasma current arises but a number of possibilities remain to be investigated. On the other hand, pulsed operation in the form of a moving-ring-reactor avoids this difficulty and may introduce other simplifications as well.

Experiments of the past several years have produced a very rapid broadening of the physics knowledge of the CT and a corresponding exploration of reactor possibilities. The next few years will hopefully continue this process as further experiments and more detailed theory develop.

## REFERENCES


1. C. W. Hartman, "Summary of U. S. Compact Torus Experiment," in these proceedings.
2. H. A. B. Bodin, A. A. Newton, Phys. Fluids 6 (1963) 1338; E. M. Little, W. E. Quinn, Phys. Fluids 6 (1963) 875.
3. W. Newcomb, Phys. Fluids 23, 11 (1980) 2296.
4. C. W. Hartman, Appendix C in W. Condit, et al., "Status Report on Mirror Alternatives," UCRL-52008, Feb. 3, 1976.
5. W. Newcomb, Phys. Fluids 23, 11, (1980) 2296.
6. C. W. Hartman, "Finite Larmor Radius Stabilized Z-Pinches," UCID-17118, April 1976.
7. H. A. B. Bodin, A. A. Newton, Phys. Fluids 6 (1963) 1338; E. M. Little, W. E. Quinn, Phys. Fluids 6 (1963) 875.

8. G. A. Carlson et al., "Conceptual Design of the Field-Reversed Mirror Reactor," Lawrence Livermore National Laboratory, Report UCRL-52467.
9. G. A. Carlson, K. R. Schultz, A. C. Smith, Jr., "Definition and Conceptual Design of a Small Fusion Reactor," Electric Power Research Institute Report ER-1045 (1979).
10. G. A. Carlson et al., "Field-Reversed Mirror Pilot Reactor," Electric Power Research Institute Report AP-1544 (1980).
11. G. H. Miley and J. G. Gilligan, Energy, Vol. 4, No. 2, 163-170 (1979).
12. V. D. Shafranov, "Plasma Equilibrium in a Magnetic Field," Reviews of Plasma Physics, Vol. 2, p. 103.
13. J. H. Hammer and H. L. Berk, Proc. of the US-Japan Joint Symposium on Compact Toruses and Energetic Particle Injection, Princeton, Dec. 1979, p. 80.
14. T. Ohkawa, Nuclear Fusion 10 (1970) 185.
15. W. C. Turner et al., Proc. Third Symposium on Physics and Technology of Compact Toroids, Los Alamos Scientific Laboratory, Dec. 1980, LA-8700-C, p. 113.
16. J. Marshall, "Coaxial Guns as Injectors of High Linear Theta Pinches," Proceedings of the High Beta Workshop at LASL ERDA-76/108, July 28-August 1, 1975, p. 470.
17. J. Hammer, private communication 1980.
18. J. Hammer, private communication 1980.
19. M. N. Rosenbluth and M. N. Bussac, Nucl. Fusion 19, 489 (1979).
20. A. C. Smith, Jr., et al., Proc. Third Symposium on Physics and Technology of Compact Toroids, Los Alamos Scientific Laboratory, Dec. 1980, LA-8700-C, p. 12.
21. R. L. Hagenson and R. A. Krakowski, Proc. Third Symposium on Physics and Technology of Compact Toroids, Los Alamos Scientific Laboratory, Dec. 1980, LA-8700-C, p. 8.
22. M. N. Bussac et al., IAEA Conference (Innsbruck 1978), Vol. II, p. 249.
23. H. H. Fleischmann, "Proc. Third Symposium on Physics and Technology of Compact Toroids, Los Alamos Scientific Laboratory, Dec. 1980, LA-8700-C, p. 31.
24. G. Bekefi, "Radiation Processes in Plasmas," J. Wiley & Sons, Inc. Published 1966, p. 180.
25. W. Bennett, Phys. Rev. 98, 1584 (1955).
26. S. Yoshikawa, Phys. Rev. Lett. 26, 705 (1971).
27. C. W. Hartman and M. A. Levine, Proc. of the US-Japan Joint Symposium on Compact Toruses and Energetic Particle Injection, Princeton, Dec. 1979, p. 68.
28. M. N. Bussac et al., IAEA Conference (Innsbruck 1978), Vol. II, p. 249.

29. H. Fleischman and T. Kammash, Nuclear Fusion 15 (1975) p. 1143.
30. Baldwin, D. E. and M. E. Rensink, Comments on Plasma Physics and Controlled Fusion IV (1978) 55.